

Standards-Compliant DM-RS Allocation via Temporal Channel Prediction for Massive MIMO Systems

Sehyun Ryu and Hyun Jong Yang, *Member, IEEE*

Abstract—Reducing feedback overhead in beyond 5G networks is a critical challenge, as the growing number of antennas in modern massive MIMO systems substantially increases the channel state information (CSI) feedback demand in frequency division duplex (FDD) systems. To address this, extensive research has focused on CSI compression and prediction, with neural network-based approaches gaining momentum and being considered for integration into the 3GPP 5G-Advanced standards. While deep learning has been effectively applied to CSI-limited beamforming and handover optimization, reference signal allocation under such constraints remains surprisingly underexplored. To fill this gap, we introduce the concept of channel prediction-based reference signal allocation (CPRS), which jointly optimizes channel prediction and DM-RS allocation to improve data throughput without requiring CSI feedback. We further propose a standards-compliant ViViT/CNN-based architecture that implements CPRS by treating evolving CSI matrices as sequential image-like data, enabling efficient and adaptive transmission in dynamic environments. Simulation results using ray-tracing channel data generated in NVIDIA Sionna validate the proposed method, showing up to 36.60% throughput improvement over benchmark strategies.

Index Terms—5G NR, Massive MIMO, Reference Signal, DM-RS, Channel Prediction, Deep Learning.

I. INTRODUCTION

The multiple-input-multiple-output (MIMO) systems [1] have been at the core of innovation since 4G LTE to enhance data throughput. However, despite its original goal, the introduction of massive MIMO has led to the challenge of increased channel dimensionality [2]. As the dimension of the channel matrix increases, both the transmission of the reference signal for channel estimation and the feedback of downlink channel state information (CSI) to the base station have become significant sources of overhead. The downlink CSI is critical for enhancing communication tasks such as *beamforming* [3], *handover* [4], and *reference signal allocation* [5]. In time division duplexing (TDD) systems, the downlink channel can be inferred from the uplink channel due to channel reciprocity. However, in frequency division duplexing (FDD) systems, CSI feedback is required [6]. As CSI feedback has become a major source of overhead in FDD systems, extensive research has been conducted to address this challenge [7].

Recently, deep learning has emerged as a breakthrough solution for reducing CSI feedback overhead and is also being

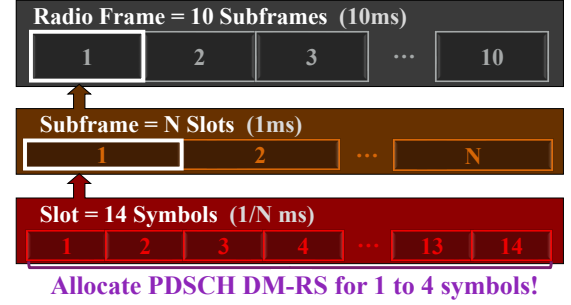


Fig. 1: The NR frame structure and its corresponding transmission timings are defined based on a 10ms radio frame, consisting of ten 1ms subframes. The number of slots per subframe, N , is flexibly determined by the numerology specified in 3GPP TS 38.211 table 4.3.2-1 [8], where $N = 2^\mu$, $\mu \in \mathbb{Z}$, and $0 \leq \mu \leq 6$. Within each slot, the PDSCH DM-RS can be configured to occupy 1 to 4 out of the 14 OFDM symbols.

discussed in the 5G Advanced standards following 3GPP Rel-18 [9]. The solutions can be broadly classified into two categories: CSI compression [10] and channel prediction [11]. We focus on channel prediction, which estimates downlink CSI from uplink CSI or data signals, even without explicit CSI feedback. The network architectures have evolved from CNNs [11] to LSTMs [12], and more recently, transformers [13]. There have also been attempts to jointly optimize beamforming and handover, the primary objectives of channel prediction. For instance, [14] proposed a deep reinforcement learning algorithm for channel prediction and beamforming, while [15] used a transformer-based approach for beamforming with predicted CSI. In terms of handover, channel quality prediction has been used to guide handover decisions [16]. However, to the best of the authors' knowledge, no prior study has explored the critical issue of reference signal allocation in conjunction with channel prediction, despite their strong interdependence.

We address the allocation of the physical downlink shared channel (PDSCH) demodulation reference signal (DM-RS) within the NR frame structure, as illustrated in Fig. 1. Among various reference signals defined in 3GPP NR, the PDSCH DM-RS plays a critical role in determining data throughput, as it directly enables the user equipment (UE) to estimate the channel for data demodulation. Moreover, unlike other reference signals transmitted over the control plane, the DM-RS is carried on the data plane alongside data symbols. The NR standard provides various configuration options for the flexible placement of 1 to 4 DM-RS symbols within each slot, the transmission time interval (TTI) of the NR frame, as detailed in Table I, offering a level of flexibility not available in previous LTE standards. This design accommodates practical

Sehyun Ryu is with the Department of Electrical Engineering, Pohang University of Science and Technology (POSTECH), Pohang, Republic of Korea (e-mail: sh.ryu@postech.ac.kr).

Hyun Jong Yang is the corresponding author and is with the Department of Electrical and Computer Engineering and the Institute of New Media and Communications, Seoul National University (SNU), Seoul, Republic of Korea (e-mail: hjyang@snu.ac.kr).

TABLE I: DM-RS positions within a 14-symbol slot duration are specified in Table 7.4.1.1.2-3/4 of 3GPP TS 38.211 [8], with $l_0 \in \{2, 3\}$ and $l_1 \in \{11, 12\}$. Only Type-A configurations are included, as Type-B applies to a special use case of mini-slot-based scheduling with fewer supported allocation patterns.

DM-RS Length	DM-RS positions			
	pos0	pos1	pos2	pos3
Single-Symbol	l_0	l_0, l_1	$l_0, 7, 11$	$l_0, 5, 8, 11$
Double-Symbol	l_0	$l_0, 10$	-	-

challenges such as mobility-induced channel aging, noise, and estimation uncertainty. The in-slot placement makes DM-RS allocation particularly important, as increasing the number of DM-RS symbols improves channel estimation accuracy at the expense of reducing transmittable data symbols, highlighting an inherent trade-off in the allocation design. Therefore, the DM-RS must be optimally allocated to balance channel estimation quality and the number of available data symbols, considering the current downlink CSI. However, as the standard does not specify which allocation to use under specific downlink CSI conditions, network operators have the flexibility to configure it based on their own channel assessments.

This paper proposes a channel prediction-based reference signal allocation method, with a focus on DM-RS, for massive MIMO systems in B5G networks. While designed with B5G scenarios in mind, the proposed method remains fully compatible with the 5G NR frame structure and is applicable under current standard specifications.

Contribution: 1) This paper introduces the concept of channel prediction-based reference signal allocation (CPRS), with a particular focus on DM-RS, as a practical approach to reducing CSI feedback overhead in massive MIMO FDD scenarios. 2) We propose a ViViT/CNN-based [17] CPRS algorithm, designed with consideration of the NR frame structure, which interprets time-varying uplink channel matrices as video data. 3) We generate ray-tracing-based channel data and perform simulations using NVIDIA Sionna [18], demonstrating the effectiveness of the proposed method.

II. SYSTEM MODEL AND PROBLEM FORMULATION

We consider a massive MIMO-OFDM communication system, focusing on a downlink scenario with UE mobility, where the BS and UE communicate based on the NR frame structure. The numbers of receive antennas, transmit antennas, and subcarriers are denoted by N_R , N_T , and N_C , respectively. The antennas at the UE receive the same transmitted signal, and the received signal at the UE for the t -th OFDM symbol in the slot and k -th subcarrier can be expressed as follows:

$$y_{t,k} = \mathbf{h}_{DL,t,k} \mathbf{v}_{t,k} x_{t,k} + \mathbf{w}_{t,k}, \quad (1)$$

where $\mathbf{h}_{DL,t,k} \in \mathbb{C}^{N_R \times N_T}$ is the downlink channel matrix associated with the t -th symbol and k -th subcarrier, $\mathbf{v}_{t,k} \in \mathbb{C}^{N_T \times 1}$ is the precoding vector, $x_{t,k} \in \mathbb{C}$ is the transmit symbol, and $\mathbf{w}_{t,k} \in \mathbb{C}^{N_R \times 1}$ denotes additive noise. Then, each t -th symbol within the slot has a distinct downlink CSI as follows:

$$\mathbf{H}_{DL,t} = [\mathbf{h}_{DL,t,1} \mathbf{h}_{DL,t,2} \cdots \mathbf{h}_{DL,t,N_C}] \in \mathbb{C}^{N_R \times N_T \times N_C} \quad (2)$$

We define the overall downlink CSI for a slot as \mathbf{H}_{DL} , which consists of the CSI matrices corresponding to all 14 OFDM symbols in the slot. It is expressed as:

$$\mathbf{H}_{DL} = \{\mathbf{H}_{DL,t}\}_{t=1}^{14} \quad (3)$$

In our system, the BS is assumed to predict \mathbf{H}_{DL} using the uplink CSI from the current slot, denoted as $\mathbf{H}_{UL} = \{\mathbf{H}_{UL,i} \in \mathbb{C}^{N_T \times N_R \times N_C}\}_{i \in I_u}$, where I_u is the set of DM-RS symbol indices in the current uplink slot. We assume that the uplink DM-RS is transmitted at four symbols per slot and $I_u = \{2, 5, 8, 11\}$. The downlink channel prediction using a predictor function $f(\cdot)$ is formulated as:

$$\hat{\mathbf{H}}_{DL} = f(\mathbf{H}_{UL}) \quad (4)$$

The BS utilizes $\hat{\mathbf{H}}_{DL}$ to identify the optimal allocation $p^* \in \mathcal{P}$, where \mathcal{P} denotes the set of possible allocation configurations from which the BS selects one to configure the next slot, in order to maximize data throughput. We refer to this process as *channel prediction-based reference signal allocation (CPRS)*, and define the corresponding optimization problem as follows:

$$p^* = \arg \max_{p \in \mathcal{P}} \left\{ R \cdot D_{\text{sent}} \cdot \left(1 - \frac{n_p}{n_s} \right) \cdot (1 - \text{BLER}) \right\}, \quad (5)$$

given $\hat{\mathbf{H}}_{DL} = f(\mathbf{H}_{UL})$, where R is the code rate, D_{sent} is the total number of bits transmitted in one slot, n_p is the number of DM-RS symbols in allocation p , $n_s = 14$ is the number of symbols within a slot, and BLER denotes the block error rate at the UE. The objective function of (5) represents the data throughput (bits per slot), following the model in [19]. We focus on the core optimization problem, excluding retransmissions as they fall outside the scope of this study. Here, R , D_{sent} , and n_s are constants for a fixed numerology and thus independent of p , while n_p , the number of DM-RS symbols, is directly determined by the allocation p . The key challenge lies in modeling the complex relationship among p , \mathbf{H}_{UL} , and the resulting BLER at the UE in the next slot.

Even if the BS accurately estimates the \mathbf{H}_{DL} , it remains challenging to determine the extent of BLER caused by channel errors in symbols between DM-RS placements. We adopt a data-driven approach to determine the relationship among p , \mathbf{H}_{UL} , BLER, and ultimately, data throughput. Utilizing neural network algorithms often applied in nonconvex optimization, we propose an end-to-end method that jointly optimizes both the channel prediction problem in (4) and the DM-RS allocation in (5), classifying optimal allocation $p^* \in \mathcal{P}$ directly from \mathbf{H}_{UL} . For the neural network-based classifier $\mathcal{F}(\cdot; \Theta)$ and estimated allocation $\hat{p}^* \in \mathcal{P}$, the proposed CPRS method is defined as:

$$\hat{p}^* = \mathcal{F}(\mathbf{H}_{UL}; \Theta) \quad (6)$$

We assume the possible allocation set \mathcal{P} follows the NR standard in Table I. Without loss of generality, to simplify our analysis in this study, we consider the typical case of $l_1 = 11$, yielding $|\mathcal{P}| = 13$ possible allocations, and apply Kronecker placement to focus on time-domain symbol allocation, as frequency-domain patterns (Type 1 and Type 2) are limited to only two fixed configurations and offer little flexibility.

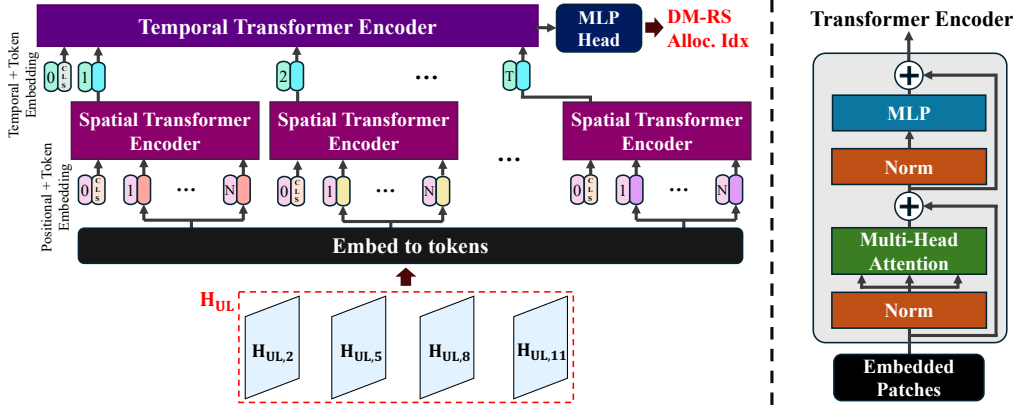


Fig. 2: The proposed ViViT-based CPRS network captures the temporal variation of uplink channel matrices \mathbf{H}_{UL} , obtained from DM-RS symbols at positions $I_u = \{2, 5, 8, 11\}$ within an uplink slot. Leveraging a transformer architecture optimized for video data, it predicts the optimal DM-RS allocation for the next slot.

III. ViViT/CNN-BASED CPRS NETWORK

Fig. 2 illustrates our proposed *ViViT-based CPRS* network, designed to predict optimal DM-RS allocations by exploiting the temporal evolution of uplink channel matrices \mathbf{H}_{UL} . We also introduce a lower-complexity CNN-based variant with the same input-output configuration, whose standard architecture is omitted for brevity.

Each $\mathbf{H}_{UL,i}$ for $i \in \{2, 5, 8, 11\}$ is first decomposed into real and imaginary parts, which are concatenated to form a multi-channel representation, then reshaped into non-overlapping patches that are flattened and embedded as tokens. Specifically, the channel matrix, originally of size $N_T \times N_R \times N_C$, is reshaped by flattening the antenna dimensions, resulting in the following input tensor \mathbf{X}_i for the network:

$$\mathbf{H}_{UL,i} \in \mathbb{C}^{N_T \times N_R \times N_C} \implies \mathbf{X}_i \in \mathbb{R}^{N_T N_R \times N_C \times 2} \quad (7)$$

This transformation enables the network to process spatial features jointly along the flattened antenna dimension, while preserving the temporal structure along the subcarrier axis N_C . Moreover, it maintains compatibility with standard convolutional operations without losing the inherent spatial correlations present in the original matrix.

We then partition \mathbf{X}_i into a set of non-overlapping patches and flatten each patch to form the initial tokens:

$$\mathbf{z}_i^{(0)} = \{\mathbf{x}_{i,1}, \mathbf{x}_{i,2}, \dots, \mathbf{x}_{i,P}\}, \quad (8)$$

where $\mathbf{x}_{i,p}$ denotes the p -th patch and P is the total number of patches. Learnable positional encodings are applied to the patch embeddings to incorporate spatial order.

a) Spatial Transformer Encoder: In the *spatial* transformer stage, each set of token embeddings $\mathbf{z}_i^{(0)}$ for a given time index i passes through a standard transformer encoder block. Concretely, let $\mathbf{z}_i^{(\ell)} \in \mathbb{R}^{P \times D}$ be the output of the ℓ -th encoder layer, where D is the embedding dimension of each token. Each encoder layer consists of multi-head self-attention (MHSA) and a position-wise feedforward network (FFN), each followed by layer normalization. The MHSA operation is defined by:

$$\text{Attention}(Q, K, V) = \text{softmax}\left(\frac{QK^\top}{\sqrt{d}}\right)V, \quad (9)$$

where Q , K , and V are linear projections of the input $\mathbf{z}_i^{(\ell-1)}$, and d is the dimensionality of each head. Multiple attention heads are concatenated to capture diverse representation subspaces. After processing all four channel matrices in a slot independently in the spatial transformer, we obtain spatially enhanced tokens for each time i .

b) Temporal Transformer Encoder: We then stack the spatially transformed tokens across four time indices and feed them into the *temporal* transformer encoder. The same MHSA and FFN blocks now operate along the temporal dimension to learn correlations across DM-RS time positions. Stacking multiple temporal attention layers allows the network to capture channel evolution over time slots.

After the temporal transformer encoder, the final token representations are pooled and passed through a multi-layer perceptron (MLP) head to predict the optimal downlink DM-RS allocation index. This prediction leverages the spatio-temporal correlations learned via the transformer's self-attention mechanism, which effectively captures long-range dependencies, to complete the end-to-end decision pipeline. The entire ViViT/CNN-based CPRS network is trained using a cross-entropy loss, aligning the model's predictions with the ground-truth optimal DM-RS allocation labels.

The total computational complexity of the proposed ViViT model is $\mathcal{O}(L \cdot (N^2 D + N D^2))$, where L denotes the number of transformer layers, N is the number of input tokens, and D is the embedding dimension. For comparison, the CNN-based baseline consists of three 3D convolutional layers, each with computational complexity $\mathcal{O}(F \cdot C \cdot K^3 \cdot H \cdot W \cdot T)$, where K is the kernel size, C the number of input channels, F the number of output filters, and $H \times W \times T$ the spatial-temporal dimensions. Based on FLOP-level complexity analysis and efficient quantization techniques such as [20], both models are expected to be deployable at the microsecond level in a slot-based real-time system with parallel implementation.¹

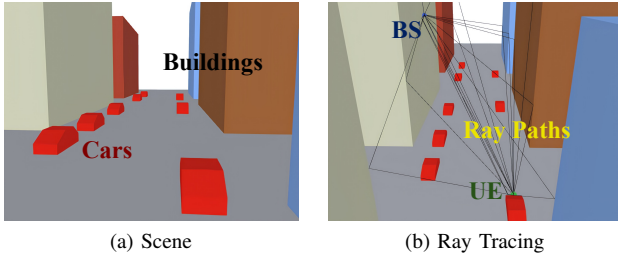


Fig. 3: Process of obtaining channel matrices via ray tracing using NVIDIA Sionna [18]. After constructing a dynamic scene that reflects movement as illustrated in (a), perform ray tracing by positioning the BS and UE as shown in (b).

A. Dataset Generation

We utilized the NVIDIA Sionna Ray Tracing to generate channel data [18], as it more accurately reflects real-world propagation characteristics and physical environments than statistical channel models. Specifically, we employed the *simple_street_canyon_with_cars* scene included in the framework. As illustrated in Fig. 3, this scenario features a road between buildings, where vehicles move along both lanes. All vehicles move at a uniform speed $v \in \{60, 65, \dots, 80\}$ km/h. The BS is installed on one of the buildings and the UE is positioned in one of the vehicles. The BS has an 8×8 antenna array, while the UE has a 2×1 antenna array, forming a massive MIMO system. We consider an FDD scenario operating in NR band n1, as specified in Table 5.2-1 of [21], using uplink and downlink carrier frequencies of 1.95 GHz and 2.14 GHz, respectively. The numerology is fixed to $N=1$, such that one subframe corresponds to a single slot. The maximum number of rays was set to 20, with a maximum ray depth of 4 and a bandwidth of 100 MHz.

For each velocity v , we obtained the uplink and downlink channel matrices for every symbol within 400 consecutive slots, each comprising 14 symbols and 64 subcarriers. Additionally, we augmented the original dataset by adding Gaussian noise with a magnitude of approximately 0.05 relative to the original channel matrices, in order to emulate practical channel estimation errors caused by uplink noise and other impairments. This augmentation generated an additional 4,000 slots. This resulted in a total dataset comprising 6,000 slots. Subsequently, for each slot, the optimal DM-RS allocation index was determined via exhaustive evaluation of all candidate configurations using Sionna link-level simulations, based on the objective function defined in (5). The dataset was then divided into training, validation, and test sets using an 8:1:1 ratio.

IV. EXPERIMENTAL RESULTS

A. Considered Schemes

- CPRS (ViViT): The proposed scheme in Section III. Our model adopts a tubelet embedding approach with patch sizes of (1,8,8), with a transformer backbone consisting of 8 encoder layers, each with 16 attention heads.

¹With $L=8$, $N=64$, and $D=192$ as in our experiments, the ViViT model requires $\sim 239.2 \times 10^6$ FLOPs. Assuming INT8 quantization on an NVIDIA A100 (624 TFLOPs), the theoretical inference time is $\sim 3.83 \mu\text{s}$. The CNN model, with fewer FLOPs, can run even faster.

TABLE II: Classification accuracy comparison of different schemes for selecting the optimal DM-RS allocation index in the next slot, evaluated over 250 test slots. The results are reported per SNR value, excluding SNRs below -5 dB where all DM-RS allocations yield zero data throughput.

Method	SNR (dB)								
	-5	-2.5	0	2.5	5	7.5	10	12.5	15
CPRS (ViViT)	99.78	99.50	100.00	99.67	99.84	99.89	100.00	99.83	99.95
CPRS (CNN)	<u>94.45</u>	<u>97.67</u>	100.00	<u>99.61</u>	99.84	<u>99.72</u>	<u>99.95</u>	<u>99.78</u>	99.95
Disjoint ([22])+[23])	72.06	74.96	50.10	50.10	50.15	31.51	25.08	25.08	25.06
DRL ([24])	13.46	12.00	45.61	42.95	31.06	52.33	48.33	43.00	43.61
Maximize Data Symbols	75.00	72.30	75.00	50.00	50.00	31.97	25.00	25.00	25.00
Random Average	7.69	7.69	7.69	7.69	7.69	7.69	7.69	7.69	7.69

*Best: **bold**, second-best: underline.

- CPRS (CNN): A CPRS scheme based on a 3D-CNN, where all \mathbf{X}_i are concatenated to form a four-channel input. The network consists of three Conv3D layers with 16, 32, and 64 filters, respectively. Each convolutional layer is followed by batch normalization and a 3D max pooling layer to reduce spatial dimensions.
- Disjoint ([22])+[23]): The downlink CSI is first predicted using a CNN-based channel predictor [22], and the DM-RS pattern is then optimized to maximize estimation accuracy, adapting [23] to comply with 3GPP standards.
- DRL ([24]): The CNN-based deep Q-network, inspired by [24], is adapted to our scenario, using an ϵ -greedy policy with $\epsilon = 0.3$, where the uplink CSI serves as the state, 3GPP-compliant DM-RS patterns define the action space, and throughput is used as the reward.
- Maximize Data Symbols: A scheme maximizing the number of data symbols transmitted by minimizing the number of DM-RS symbols per slot ($n_p = 1$).
- Random Average: A scheme selecting all possible DM-RS allocations with equal probability. In performance comparisons, the average performance over all possible allocations is considered.
- Best: The ground-truth DM-RS allocation that achieves the optimal data throughput obtained through simulations.

B. Performance Comparison

We analyzed the classification accuracy of each scheme in selecting the optimal DM-RS allocation index for the next slot across a range of SNR values, from very low to high (i.e., $\{-10, -7.5, \dots, 15\}$ dB). As shown in Table II, the proposed algorithm, CPRS (ViViT), achieves the highest classification accuracy across all SNR values, with performance consistently approaching 100%. In the Disjoint approach, although the CP network initially achieved accurate downlink channel prediction (NMSE of -8.42 dB) and the DM-RS pruning network attained over 98% test accuracy based on the perfect downlink CSI, the accumulation of errors from the CP module ultimately resulted in significant performance degradation. The DRL method, requiring a clearer understanding of the complex relationship between uplink CSI and throughput, converged to a lower overall performance compared to CPRS.

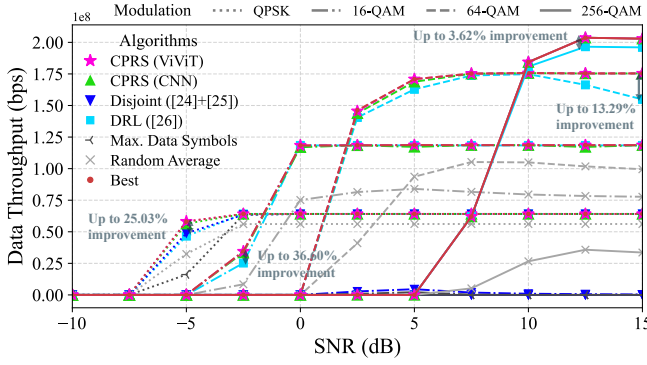


Fig. 4: Average data throughput achieved by each scheme's DM-RS allocation, evaluated over 250 randomly selected sample slots. The throughput gain of the proposed CPRS algorithm is shown relative to the second-best benchmark.

The key performance indicator at the UE is data throughput, as shown for each scheme in Fig. 4. CPRS (ViViT) achieves the highest performance across the entire SNR range and modulation orders, consistently approaching the optimum with errors between 0% and 0.48% relative to the best achievable throughput. Compared to the second-best benchmark, CPRS (ViViT) yields up to 36.60% throughput gain, and up to 13.29% gain in the saturation region under 64-QAM. CPRS (CNN) ranks second overall, with average throughput 0% to 2.60% lower than CPRS (ViViT). Other baseline methods struggle with fine-grained DM-RS allocation at higher modulation orders, with the Disjoint approach showing a BLER of 1 under 256-QAM, resulting in zero throughput and emphasizing the need for effective DM-RS design. These results highlight the conceptual validity and effectiveness of CPRS, which jointly optimizes channel prediction and DM-RS allocation.

V. CONCLUSION

In this paper, we introduced the concept of channel prediction-based reference signal allocation (CPRS) as an effective approach to reducing CSI feedback overhead in massive MIMO FDD scenarios. We proposed a ViViT/CNN-based CPRS algorithm that allocates DM-RS by learning spatial-temporal patterns from time-varying uplink channel matrices, effectively capturing the dynamics of wireless channels. Simulation results using ray-tracing channel data from NVIDIA Sionna validated the proposed method, demonstrating superior performance over benchmark strategies with up to 36.60% throughput improvement. This work lays the groundwork for future research on channel prediction-driven optimization of reference signals beyond DM-RS, including practical extensions to B5G scenarios and joint design with beamforming under diverse mobility and channel conditions.

REFERENCES

- [1] D. Gesbert, H. Bolcskei, D. Gore, and A. Paulraj, "Outdoor mimo wireless channels: models and performance prediction," *IEEE Transactions on Communications*, vol. 50, no. 12, pp. 1926–1934, 2002.
- [2] L. Lu, G. Y. Li, A. L. Swindlehurst, A. Ashikhmin, and R. Zhang, "An overview of massive mimo: Benefits and challenges," *IEEE Journal of Selected Topics in Signal Processing*, vol. 8, no. 5, pp. 742–758, 2014.
- [3] S. Jafar, S. Vishwanath, and A. Goldsmith, "Channel capacity and beamforming for multiple transmit and receive antennas with covariance

- feedback," *IEEE International Conference on Communications*, vol. 7, pp. 2266–2270 vol.7, 2001.
- [4] A. Tolli, M. Codreanu, and M. Juntti, "Cooperative mimo-ofdm cellular system with soft handover between distributed base station antennas," *IEEE Transactions on Wireless Communications*, vol. 7, no. 4, pp. 1428–1440, 2008.
- [5] X. Cai and G. Giannakis, "Adaptive psam accounting for channel estimation and prediction errors," *IEEE Transactions on Wireless Communications*, vol. 4, no. 1, pp. 246–256, 2005.
- [6] D. J. Love, R. W. Heath, V. K. N. Lau, D. Gesbert, B. D. Rao, and M. Andrews, "An overview of limited feedback in wireless communication systems," *IEEE Journal on Selected Areas in Communications*, vol. 26, no. 8, pp. 1341–1365, 2008.
- [7] J.-C. Shen, J. Zhang, K.-C. Chen, and K. B. Letaief, "High-dimensional csi acquisition in massive mimo: Sparsity-inspired approaches," *IEEE Systems Journal*, vol. 11, no. 1, pp. 32–40, 2017.
- [8] ETSI, "Physical channels and modulation," 650 Route des Lucioles, France, TS 138.211 V18.4.0, pp. 12–132, Oct. 2024.
- [9] 3GPP, "New si: Study on artificial intelligence (ai)/machine learning (ml) for nr air interface," RP-213599, Moderator (Qualcomm), Tech. Rep., Dec. 2021.
- [10] C.-K. Wen, W.-T. Shih, and S. Jin, "Deep learning for massive mimo csi feedback," *IEEE Wireless Communications Letters*, vol. 7, no. 5, pp. 748–751, 2018.
- [11] J. Wang, Y. Ding, S. Bian, Y. Peng, M. Liu, and G. Gui, "Ul-csi data driven deep learning for predicting dl-csi in cellular fdd systems," *IEEE Access*, vol. 7, pp. 96 105–96 112, 2019.
- [12] I. Helmy, P. Tarafder, and W. Choi, "Lstm-gru model-based channel prediction for one-bit massive mimo system," *IEEE Transactions on Vehicular Technology*, vol. 72, no. 8, pp. 11 053–11 057, 2023.
- [13] T. Zhou, X. Liu, Z. Xiang, H. Zhang, B. Ai, L. Liu, and X. Jing, "Transformer network based channel prediction for csi feedback enhancement in ai-native air interface," *IEEE Transactions on Wireless Communications*, vol. 23, no. 9, pp. 11 154–11 167, 2024.
- [14] M. Chu, A. Liu, V. K. N. Lau, C. Jiang, and T. Yang, "Deep reinforcement learning based end-to-end multiuser channel prediction and beamforming," *IEEE Transactions on Wireless Communications*, vol. 21, no. 12, pp. 10 271–10 285, 2022.
- [15] H. Jiang, M. Cui, D. W. K. Ng, and L. Dai, "Accurate channel prediction based on transformer: Making mobility negligible," *IEEE Journal on Selected Areas in Communications*, vol. 40, no. 9, pp. 2717–2732, 2022.
- [16] P. Skaba, Z. Becvar, P. Mach, and I. Guvenc, "Coordinated machine learning for handover in mobile networks with transparent relaying uavs," *2024 IEEE International Conference on Communications Workshops (ICC Workshops)*, pp. 1761–1766, 2024.
- [17] A. Arnab, M. Dehghani, G. Heigold, C. Sun, M. Lučić, and C. Schmid, "Vivit: A video vision transformer," *Proceedings of the IEEE/CVF International Conference on Computer Vision (ICCV)*, pp. 6836–6846, October 2021.
- [18] J. Hoydis, S. Cammerer, F. Ait Aoudia, A. Vem, N. Binder, G. Marcus, and A. Keller, "Sionna: An open-source library for next-generation physical layer research," *arXiv preprint*, Mar. 2022.
- [19] R. N. Das, P. Bhuvaneshwari, and S. Ezhilarasi, "Throughput analysis of a lte system for static environment," pp. 1–6, 2015.
- [20] N. Zmora, H. Wu, and J. Rodge, "Achieving fp32 accuracy for int8 inference using quantization aware training with nvidia tensorrt," <https://developer.nvidia.com/blog/achieving-fp32-accuracy-for-int8-inference-using-quantization-aware-training-with-tensorrt/>, 2021, NVIDIA Developer Blog.
- [21] ETSI, "User equipment (ue) radio transmission and reception; part 1: Range 1 standalone," 650 Route des Lucioles, France, TS 138.101-1 V18.7.0, pp. 34–36, Nov. 2024.
- [22] Y. Yang, F. Gao, Z. Zhong, B. Ai, and A. Alkhateeb, "Deep transfer learning-based downlink channel prediction for fdd massive mimo systems," *IEEE Transactions on Communications*, vol. 68, no. 12, pp. 7485–7497, 2020.
- [23] M. B. Mashhadi and D. Gündüz, "Pruning the pilots: Deep learning-based pilot design and channel estimation for mimo-ofdm systems," *IEEE Transactions on Wireless Communications*, vol. 20, no. 10, pp. 6315–6328, 2021.
- [24] K. Kim, Y. K. Tun, M. S. Munir, W. Saad, and C. S. Hong, "Deep reinforcement learning for channel estimation in ris-aided wireless networks," *IEEE Communications Letters*, vol. 27, no. 8, pp. 2053–2057, 2023.